Comparison of the properties of silica aerogel doped with two different laser dyes: Crystal violet and Rhodamine B

Samah S. Ahmed, Israa F. Al-Sharuee*

Dept. of Physics, College of Science, Mustansiriyah University
Baghdad, Iraq

** Corresponding author: i81f54@uomustansiriyah.edu.iq*

Abstract

In this paper, silica aerogel was doped with two laser dyes, Crystal violet and Rhodamine B, dissolved in ethanol. All samples were prepared in two different ways, with different concentrations and compared with non-doped prepared aerogel. The first way is the modification after the samples are converted to gel. The second way, the modification procedure, starts by adding the modified solution to the sol. TEOS was used as a precursor in two-step acid-base catalysis, and the silanol group trimethylchlorosilane + n-hexane was used as a surface modification. Fourier-transform infrared spectroscopy, field emission scanning electron microscope, X-ray diffraction, nitrogen adsorption-desorption isotherm, and contact angle measurements compared the characterization and structural properties of the two dyes. Results indicate that crystal violet gives better than Rhodamine B, as the contact angle measurement was 153°, total pour volume was 1.066 cm^3/gm and the surface area was more significant than 970 m^2/gm. While for Rhodamine B, the maximum contact angle was 146°, and the largest surface area was 899 m^2/gm. And total pour volume was 1.6 cm^3/gm.

Keywords: Ambient pressure; crystal violet; doped aerogel; laser dyes; Rhodamine B

1. Introduction

Silica aerogel is a one-of-a-kind three-dimensional nanoporous material. These lightest and lowest-density solid materials have been identified so far in the world (D. Huang, Guo, Zhang, & Shi, 2017). Aerogels are materials with nano-sized pores. low density (0.003-0.35), high porosity (over 90%), and a large surface area (400-1000) m^2/gm (Sui, Liu, Lajoie, & Charpentier, 2010; Wiener, Reichenauer, Braxmeier, Hemberger, & Ebert, 2009). These features of aerogels make them of great interest to scientists for study and application in various fields. Aerogels are being used in a variety of applications, including air filtration and water purification (Israa F Al-sharuee & Mohammed, 2019; Maleki, 2016), thermal insulation (Israa F Al-sharuee, 2019), catalysts and catalyst supports, gas filters and gas storage materials, and conductive and dielectric materials (Al-Mothafer, Abdulmajeed, & Al-Sharuee, 2021; Anderson & Carroll, 2011). In general, the synthesis of aerogel consists of two basic stages: (1) gel production using the sol-gel technique and (2) drying

using supercritical or ambient pressure (Pierre & Rigacci, 2011). Laser dyes have been used as an aid to improve the structural properties of silica gel. The development of sol-gel technique provides the mixing of inorganic and organic components at the nanometer scale (Cao *et al*., 2018). The supercritical drying process consumes so much energy and is so risky that it is difficult to put it into practice and commercialize it. As a result, silica aerogel must be manufactured. at a low cost, using an ambient pressure drying approach. Currently, the most commonly used methods for measuring ambient pressure are: Network reinforcement and solvent exchange are two aspects of drying (Guo *et al.*, 2021). Wet gels have a surface modified by (Chandradass, Kang, & Bae, 2008; Rao, Nilsen, & Einarsrud, 2001; Shi, Wang, & Liu, 2006). They established a surface modification method that used a mixture of trimethylchlorosilane (TMCS) and n-hexane as the surface modification solution to produce hydrophobic silica aerogel without using a solvent exchange. A reduction in water adsorption was observed when hydrolytically stable Si–OR (R = alkyl or aryl groups) were substituted for Si-OH groups, resulting in hydrophobic aerogels (Yun, Luo, & Gao, 2014). Shan Yun proposed a novel ambient pressure drying (APD) method for drying precursor silica microspheres generated via a water-in-oil suspension process utilizing methyltrimethoxysilane (MTMS). The aerogels are superhydrophobic have a contact angle of up to 172, a good absorption, and recyclability for organic liquids and oils (Yun *et al*., 2014). Ming Li, Xu, Hai, & Zheng. Using a new co-precursor technique, prepared low-density and hydrophobic silica aerogels that were dried at ambient pressure. The starting ingredients were organic tetraethoxysilane (TEOS) and inorganic aqueous alkaline silica, with trimethylchlorosilane (TMCS) as the surface modification agent. That could be used to make solid silica aerogels that don't have cracks and have high porosity. (Li, Jiang, Xu, Hai, & Zheng, 2016). Xia Huang, Liu, Shi, Yu, & Liu. A novel "Cs0.33WO3/SiO_2" composite aerogel was created by ambient pressure to efficiently remove Rhodamine B from water, using hexamethyldisilane-HCl for the surface modification of the wet gel. The as-prepared compound aerogels displayed high specific surface area, with 265–465 m^2/g, and pore volume, with 1.11–1.86 cm^3/g. The adsorption mechanism of Rhodamine B on the "$Cs0.33WO_3/SiO_2$" compound aerogels with different content was studied using kinetic adsorption models. The compound aerogels displayed admirable absorptivity and photocatalytic degradation performance and higher recovering efficiency for the pollutant Rhodamine B (X. Huang, Liu, Shi, Yu, & Liu, 2016). Israa F. Al-Sharuee, W. Twej. investigated the effect of doping silica aerogel with CuCl2 via two-step acid-base catalysis at ambient pressure. It has been demonstrated that the doping method improves the hydrophobic properties of aerogels by lowering their density, resulting in smaller particle sizes and a more homogeneous surface (Al-Sharueez & Twej, 2017). Another study showed the effect of one type of rhodamine (6G) dye in different concentrations on improving some properties of silica aerogel (Israa F AL-Sharuee, 2021).

This study doped silica sol with two laser dyes to produce hydrophobic aerogel with Rhodamine B and crystal violet. By creating each dye in two different ways and comparing them with no doped silica aerogel sample, this novel material offers tremendous potential in magneto-optical materials and biomedical applications.

2. Experimental procedures

2.1 materials

Tetraethoxysilane (TEOS) with a purity of 98% Sigma-Aldrich (Germany), Trimethylchlorosilane (TMCS) with a purity of > 98% TCI (Japan), n-Hexane with a purity of > 98% CHem-LAB (Belgium), ethanol absolute with a purity of > 99% Schariau (Spain), Crystal Violet dye SCRC (India), Rhodamine B SCRC (India), Thoma Baker (India), Ammonia Solution (NH4OH) CDH (India). Hydrochloric acid (HCl) 35-38% Thoma Baker (India).

2.2 Samples preparation and characterization

All aerogel samples were configured for two different types of laser dyes, as shown in the schematic diagram in Figure 1.

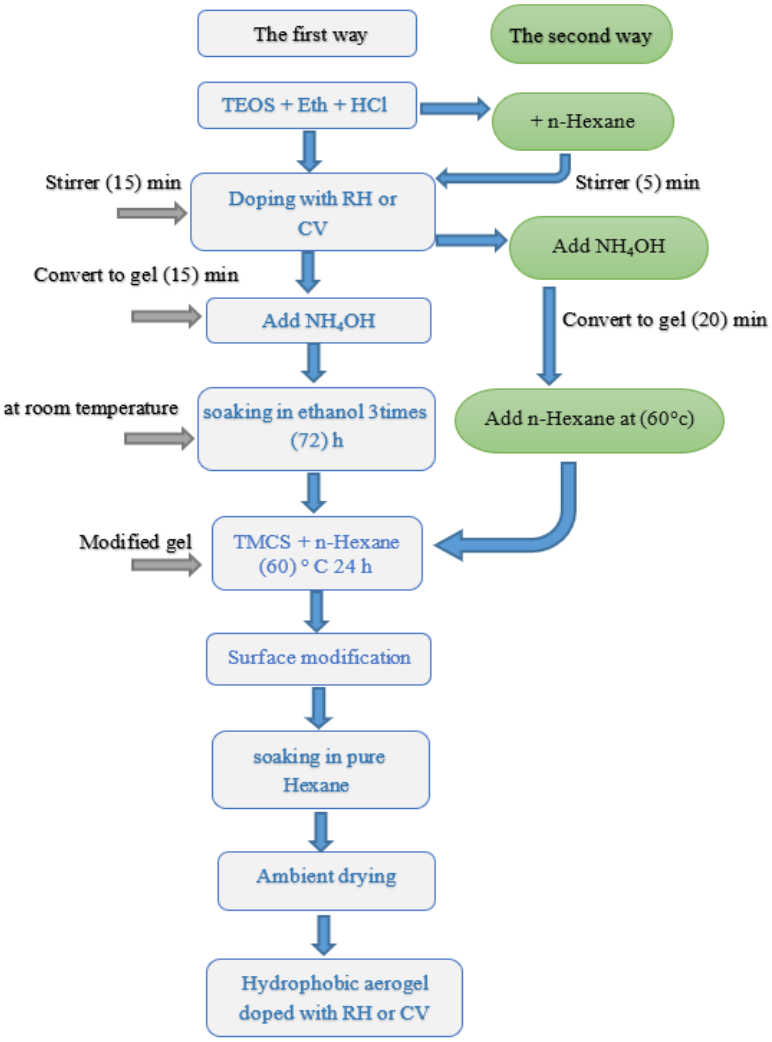

Fig. 1. Schematic diagram of the preparation of silica aerogel doped with Rhodamine B (RH) or crystal violet (CV) by ambient pressure drying by two different methods

Two different methods made the prepared samples. In the first method, an amount of one of the two dyes was mixed at a concentration of 10^{-2} g/cm^3, and this was a two-step procedure using an acid-base catalyst. The first step is to prepare condensed silica (CS) by mixing TEOS: Eth: HCl 0.1M in 1:5:0.2 molar ratio, then different amount (0.5, 1, 1.5, 2) ml of one of the two dyes is added to the CS, followed by the base catalysis. NH_4OH 0.5 M was used to convert the sol to gel after 15 minutes, then aged for 2 hours twice, and surface modification was done with TMCS and n-Hexane for 24 hours at 60°C, respectively. Then add n-Hexane twice for 24 hours each time (the amount of added n-hexane was covered by twice the modified gel volume); then wrap the holder in sulfone and make a few tiny holes. Allow the sample to dry at ambient pressure for 72 hours, then bake it at 120 degrees for 10 minutes to get a hydrophobic silica aerogel. In the other method, the samples were formed by taking a concentration of (0.5, 2) ml of both dyes. The second method is the same; the difference was by adding 5ml of n-hexane to every 5ml of CS before it turned into a gel. This procedure was done at a temperature of 60 ˚C. The sample prepared without doping is prepared in the same procedure as doped samples (RH1and CV1) but without adding the dye.

The density (ρ) of the prepared silica aerogel samples was determined by the measurement of the mass to volume ratio (ρ=m\v), where m is the sample's mass and v is the volume. The volume was calculated by measuring the radius (R) and height (h) of the sample, and considering the sample has a cylindrical shape, so the volume was calculated from the relationship ($v = \pi R^2 h$). The X-ray diffraction examination was used to observe the amorphous structure of silica aerogels in the range of 0 - 60 degrees using (GaliPIX^{3D} X-ray Detector | 2D Hybrid Pixel XRD Detector) using Cu K radiation (1.5406). The changes in surface characteristics of silica aerogel caused by TMCS were identified using Fourier Transform Infrared Spectroscopy (FTIR) (Bruker FTIR Spectrometer ALPHA II, USA). The surface morphology of the aerogel samples was investigated using a Field Emission Scanning Electron Microscope (FESEM) equipped with a FESEM EBSD Device (ZEISS SIGMA VP). The textural properties of the aerogels were investigated using a surface analyzer and a typical N2 gas adsorption method (BELSORP-mini II). BET analysis calculated the surface area from the amount of N2 gas adsorbed at various partial pressures (0.01p/p01). The water drop (3 μ) was placed on the top surface of a sample to determine its hydrophobicity, and the contact angle (θ) was calculated using the equation (1) when the drop's height (h) and width (w) were known (De Nicola *et al*., 2015).

$$\theta = 2\tan^{-1}\frac{2h}{w} \qquad (1)$$

3. Results and discussion

Table 1. Some of the physical properties of silica aerogel doped with crystal violet and Rhodamine B dye

Type of sample	Amount of dye (ml)	surface area (m^2/g)	Mean pore diameter (nm)	Total pore volume (cm^3/g)	V_m (cm^3/g)	Average Particle size nm	Density g/cm^3	Contact angle θ
CV1	0.5	944	3.5	4.4	204	29.76	0.247	151.75
	1	935	4.1	3.1	188	33.09	0.272	143.36
	1.5	920	4.9	2.90	200	38.62	0.284	147.98
	2	903	12.138	2.742	207	45.49	0.258	145.58
CV2	0.5	970	13.93	3.37	222	42.87	0.087	153.18
	2	754	5.653	1.066	173	53.35	0.135	146.72
RH1	0.5	899	13.54	3.65	172	29.27	0.238	146.07
	1	890	11.79	3.01	166	35.91	0.285	138.48
	1.5	883	10.02	2.45	185	43.8	0.240	140.44
	2	875	9.926	2.17	201	53.13	0.298	136.51
RH2	0.5	762	15.32	2.92	175	23.54	0.081	137.99
	2	689	9.39	1.61	158	63.47	0.166	134.09

Aerogel doped with crystal violet and Rhodamine B in different concentrations were prepared in two different ways. From table 1, the difference between the two methods is obvious; in the first way, after repeated washing with ethanol, a part of the dye was lost, so that its concentration decreased, and this indicates that the dye was not preserved in the internal structure of the silica gel. In a second way, hexane was added to the samples before they were converted into gels, resulting in the dye being retained in the silica network. The behavior of dye in non-polar solutions suggests that the solvent interaction around the dye cation is lessening as the solvent molecules self-associate (Shen *et al*., 2021). In addition to dyes made as catalysis for modifying the converted gel through adding enhancements to the characterization of the surface silica compared with the non-doped product (Agergaard, Sommerfeldt, Pedersen, Birkedal, & Daasbjerg, 2021). As a result, the surface area, pour volume, and average pour diameter are reduced. The obtained values found that grafting with crystal violet gave the best results compared to Rhodamine B, as shown in table 1.

3.1 FTIR analysis

Figure 2 (a- e) shows the FT-IR spectra of silica aerogels doped with RH and CV, respectively, and (e) shows no doped samples. Generally, there are no clear peaks that can be attributed to the dyes in the FTIR spectrum. Many researchers confirmed this by conducting investigations and

concluding that many dyes were in the silica network, the bands attributable to dye laser were difficult to detect, and the bands attributable to silica were not affected in the spectrum of dye/SiO_2 hybrid fibers. Studies confirmed this result, found the homogeneous distribution of dye laser in a silica matrix could have good environmental stability (Cao *et al.*, 2018; Wang *et al.*, 2012). The strong peaks at 1347 cm^{-1} and 462 cm^{-1} were caused by Si–O–Si vibrations, which were seen in all samples. The weak peak at 3621cm^{-1},1740 cm^{-1} is attributed to (O-H) because the dye was used as catalysis for modification by replacing the hydroxide band with an alkyl group, and the surface chemical modification on dye-doped aerogel was successful. (Illescas & Mosquera, 2011; Mosquera, de los Santos, & Rivas, 2010).Stretching and bending of Si-CH_3 were represented by peaks at 3283 cm^{-1}, 1593 cm^{-1}, and 1022 cm^{-1}. The peak at 1162 cm^{-1} is attributable to the stretching of Si-OH. At the same time, Figure 2 (b) shows the doped silica aerogel with crystal violet. The bands are centered at 1306, 895, and 456 cm^{-1}, which are attributed to the symmetric, asymmetric, and deformation vibrations for Si–O–Si bonds (Raissi, Younes, & Ghorbel, 2010), are present in all spectra since the backbone of silica aerogel is constituted of silica. Peaks of Si-CH_3 bending stretching were shown at 3285, 1588, and 1013 cm^{-1}, respectively. Compared to doped and no-doped, the peak attributed to the Si-OH at (1165) cm^{-1} was significantly lowered with the following modification of TMCS/n-Hexane. At the same time, the peaks assigned to the H-OH lie at (3517,1685) cm^{-1} are very weak, while they appear in Figure 2 (e) (Berardi & Zaidi, 2019). The second method in which samples were prepared is represented in Figure 2 (c, d). In Figure 2 (c), the observed bands at 1065 and 451 cm^{-1} are allied to Si–O–Si stretching vibrations. The weak peaks at 3580 cm^{-1} and 1540 cm^{-1} arose from the stretching and bending of H-OH. On the other hand, the weak peaks of around 2988 cm^{-1},1258 cm^{-1} and 847cm^{-1} were assigned to the CH_3 terminal, which also originates from the modified silica surface TMCS. It can be inferred that adding n-hexane to the sol before converting it to gel has a significant impact on silica surface modification and that at low concentrations, the hydrophobicity property improves, as seen by the contact angle values in the table 1. In Figure 2 (d), due to Si–O–Si bands, there are noticeable strong peaks at 1068 cm^{-1} and 447 cm^{-1}. This trough becomes less noticeable as the dye concentration rises. Peaks of Si-CH_3 bending stretching were seen at 2969 cm^{-1}, 1256 cm^{-1}, and 847 cm^{-1}. At the same time, the H-OH peaks are located at (3651,1543) cm^{-1}. Furthermore, the peak due to the Si-OH at (950) cm^{-1} was significantly lowered with the following modification of TMCS/n-Hexane, as seen in the figures (Linhares, de Amorim, & Durães, 2019). The hydrophobic groups (alkyl) replaced the hydrophilic ones due to the high effect of a changed solution (silanol groups).

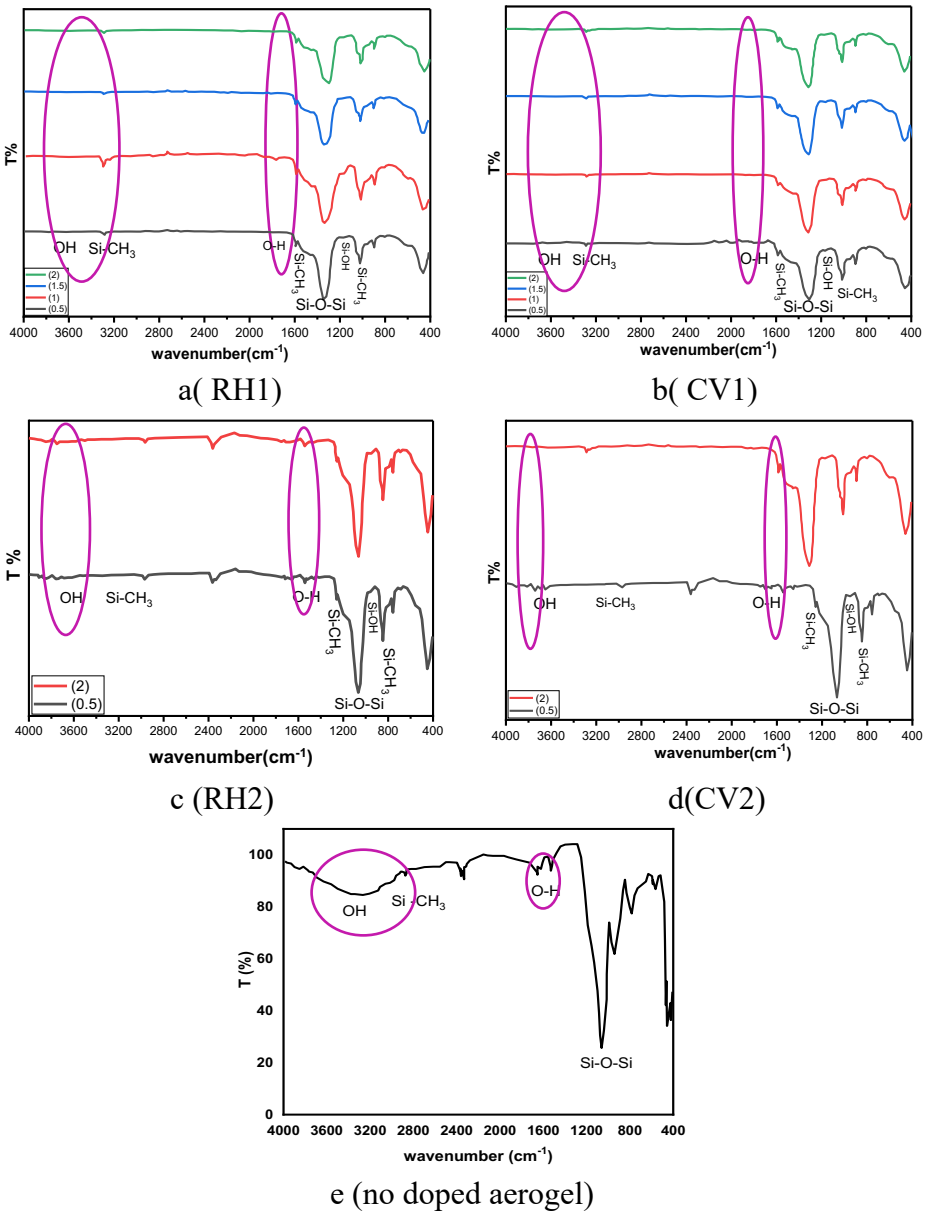

Fig. 2. FTIR spectrum for silica aerogel doped and prepared in different ways, a & b doped with Rhodamine B (RH1) and crystal violet (CV1) in the first method, c & d Rhodamine B (RH2) and crystal violet (CV2) doped with second method respectively and (e) no doped aerogel

3.2 X-Ray diffraction

Figure 3: The X-ray diffraction patterns of silica doped with Rhodamine B, crystal violet, and no doped are shown in a, b, and c. There are no X-ray diffraction peaks due to the silica's structural nature (amorphous). After vaccination, it was found that laser dyes did not affect this nature. Doped samples are generated using two distinct methods with the same amount of addition (2 mL). Small angle XRD patterns with large diffraction peaks were used. The compound XRD graph is depicted for RH samples, and ranges from 2θ equal to 12° to 27°. Another strong peak is observed at 2θ =

5.013°, which is related to the nature of the porous material and is measured. Figure 3 b. shows samples of silica doped with crystal violet. In the XRD diagram, amorphous silica is responsible for a very wide fracture extending from 2θ equals 12° to 26°. XRD patterns with smaller angles and large contrast peaks were used to show the presence of a co-organized structure in a mesoporous material (Al-Azmi, 2021; Aqeel, Greer, & Bumajdad, 2018). All the results of the samples indicated that they are highly transparent because they contain a lot of silica and allow a lot of light to pass through. The XRD pattern of silica aerogel, which was not doped, presented a broad, featureless XRD peak at a low diffraction angle, except for the broadband at 12-27 degrees, which corresponded to the amorphous state of silica (Ren, Li, Chen, Hu, & Xue, 2007).

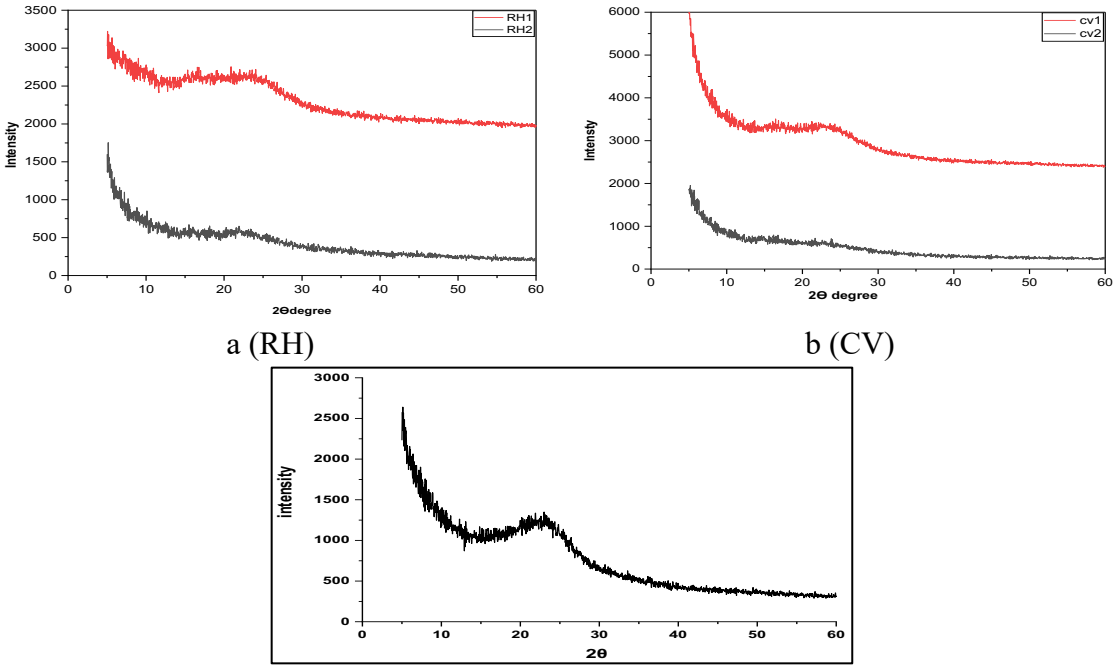

a (RH) b (CV)

(c) no doped

Fig. 3. XRD silica doped in (a) Rhodamine B and (b) Crystal Violet and (c) no doped

3.3 FESEM and EDS analysis

Figure 4 (a, b, c, d) shows FESEM of Rhodamine B and crystal violet samples were generated by two different methods (the amount of dye added to the sol was 2 ml). All silica aerogel samples at different magnifications contain a three-dimensional network produced by nanometer-sized silica particles, resembling a string of pearls or small balls. Seen noticed a smooth surface, but no swimming pools are quite as nice as that. It was discovered that when n-hexane (RH2 and CV2) was added before morphogenesis, the average particle size was larger; this was then returned to retain the molecular pigment in the silica network. On the other hand, the dye is soluble in non-polar or slightly polar organic solvents. The two preparation methods show an inhomogeneous microstructure, as large pores among the silica fractions. This means that Rhodamine-impregnated silica aerogel and crystal violet have no negative effect on their homogeneous properties. Elemental analysis of surfaces is modeled in SEM using energy dispersive spectroscopy (EDS).

Qualitative analysis of Si, O, C, N, and Cl samples reveals that for all samples, as shown in Figure 4.

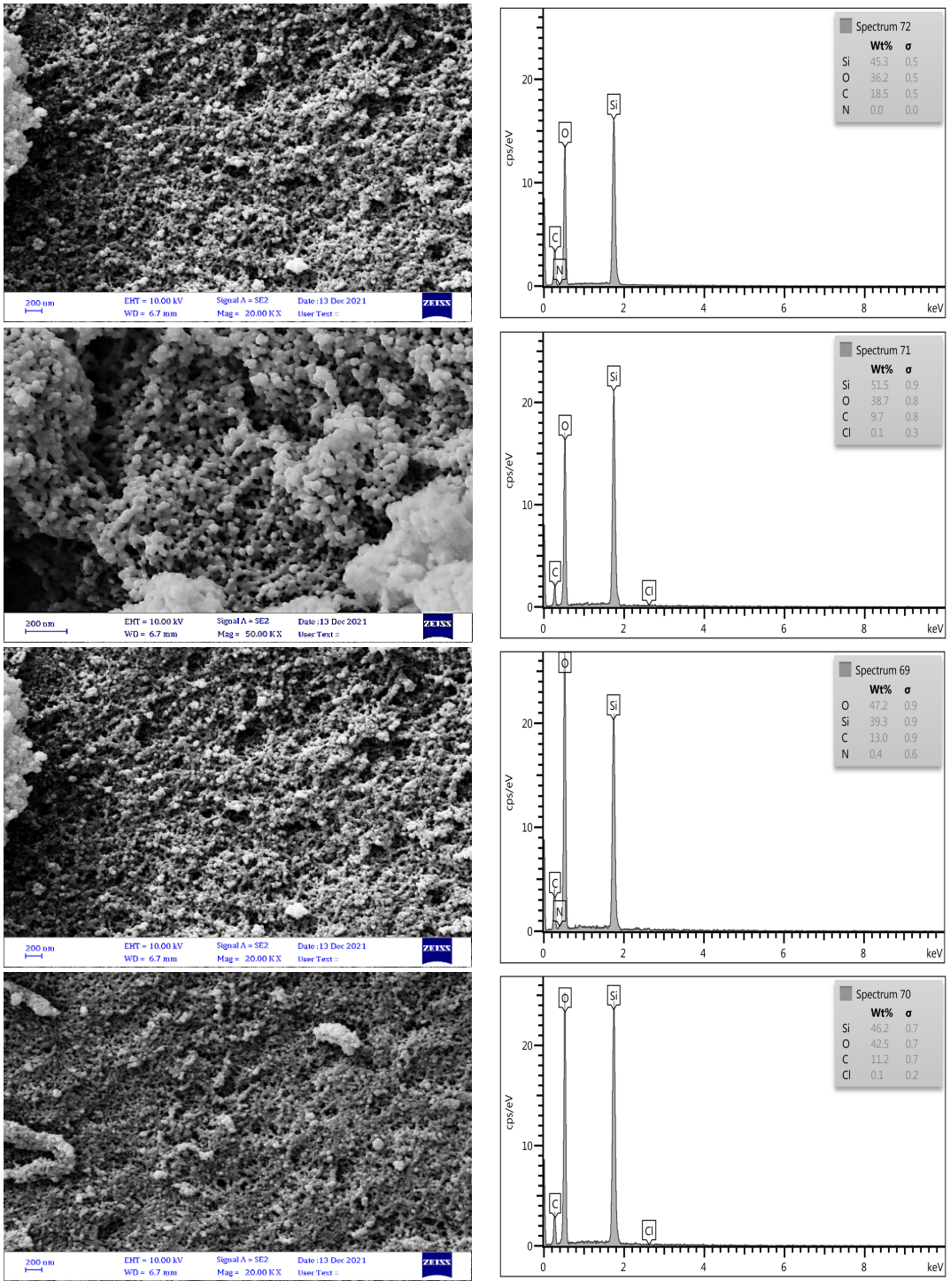

Fig. 4. FESEM image and EDS for the sample of aerogel doped with Rhodamine B and crystal violet in the first method (a, b) and second method (c, d)

3.4. Nitrogen adsorption-desorption diagram (BET)

Figure 5 shows the isotherms for N2 adsorption from aerogels for samples prepared using both methods (the amount of dye added in the first way was only 2 ml for samples RH1 and CV1, and 0.5, 2 ml for samples prepared using the second method, RH2 and CV2). The Type II adsorption-desorption isotherm was seen in all aerogel samples, indicative that the aerogels produced in this study are mesoporous. When n-hexane is added to silica sol made in the second way, the isothermal type of hexane doped with (CV2 or RH2) is generated. It is identical to the control aerogel synthesized compared to the RH1 or CV1 synthesized in the first method. Figure 5 shows the hysteresis loop (RH1, CV1, RH2 (0.5), CV2 (0.5)). More complicated pore structures with important network effects produce Type H2 hysteresis loops. The H2(a) loop's unusually steep desorption branch can be attributed to either pore-blocking/percolation in a narrow range of pore necks or cavitation-induced evaporation. Many silica gels, porous glasses, and ordered mesoporous materials contain H2(a) loops. Figure 5 RH2 (2 ml) shows an example of this. Additionally, the H2-type ring (b) is linked to the clogged pores, yet the width of the neck's size distribution is now noticeably larger. This hysteresis can be shown in a variety of ways. After hydrothermal treatment, rings were detected in medium-celled silica foam and some medium-porous silica. Figure 5 CV2 (2 ml) consists of type H3 and is given by non-rigid aggregates of plate-like particles, but also if the pore network consists of macrospores that are not filled with pore condensate (Štengl, Bakardjieva, Šubrt, & Szatmary, 2006). The Type H3 loop has two distinctive characteristics: (i) The adsorption branch has a Type II isotherm appearance. (ii) The lowest point of the desorption branch loops is the p/p0 caused by cavitation.

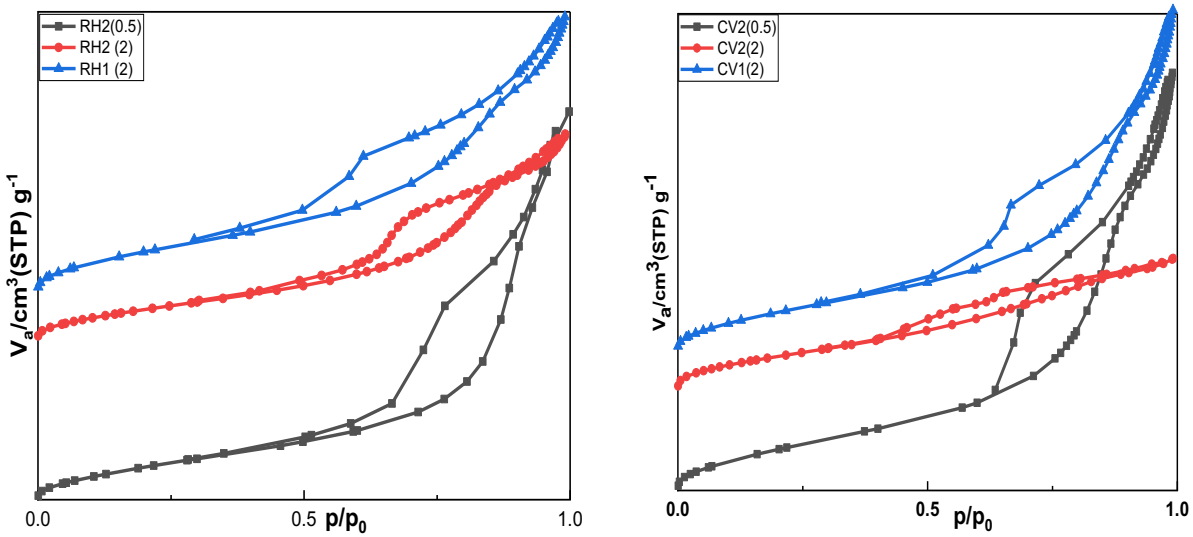

Fig. 5. N2 adsorption-desorption isotherms for doped silica aerogels: a) Rhodamine B doped, b) crystal violet doped, in two different methods

3.5 contact angle measurement

The contact angle between a water droplet supported on the outer surface and the surface under study can be used to determine the hydrophobic properties. From contact angle measurement of the aerogels, while keeping them in the same environment, the photographic images show the difference between all samples doped and those not doped. More transparency was evident in the sample without the addition of dye. This is expected since silica is closer to glass in its spectral properties. It was possible to evaluate the effect of doping and adding n-Hexane to silica sol on the water resistance of aerogels. The amount of dye (0.5, 1, 1.5, and 2 ml) made a difference in the contact angle of the aerogel samples created by the first method, RH1, and CV1, whereas the amount of dye made a difference in the contact angle of the aerogel samples prepared by the second method, RH2, and CV2 (0.5, 2 ml). In this study, two parameters affect the hydrophobicity property: the first is the amount of dye used, which indicates its concentration, and the second is the preparation environment. Because of the nature of the dye's structure, which consists of carbon and chloride molecules, it has been shown that increasing the dye concentration can improve the contact angle. In addition, the pH of the sol was 8, indicating a base preparation environment. In alkaline solutions, nucleophilic hydroxyl ions attack the dye's electrophilic central carbon, which replaces the hydroxyl ions with alkyl groups (Krause & Goldring, 2019). Table 1 and Figures 6 show that the results of contact angle and surface area, which were obtained by crystal violet, are much better than the results of Rhodamine B. The Figures 6 shows both ways of preparing samples.

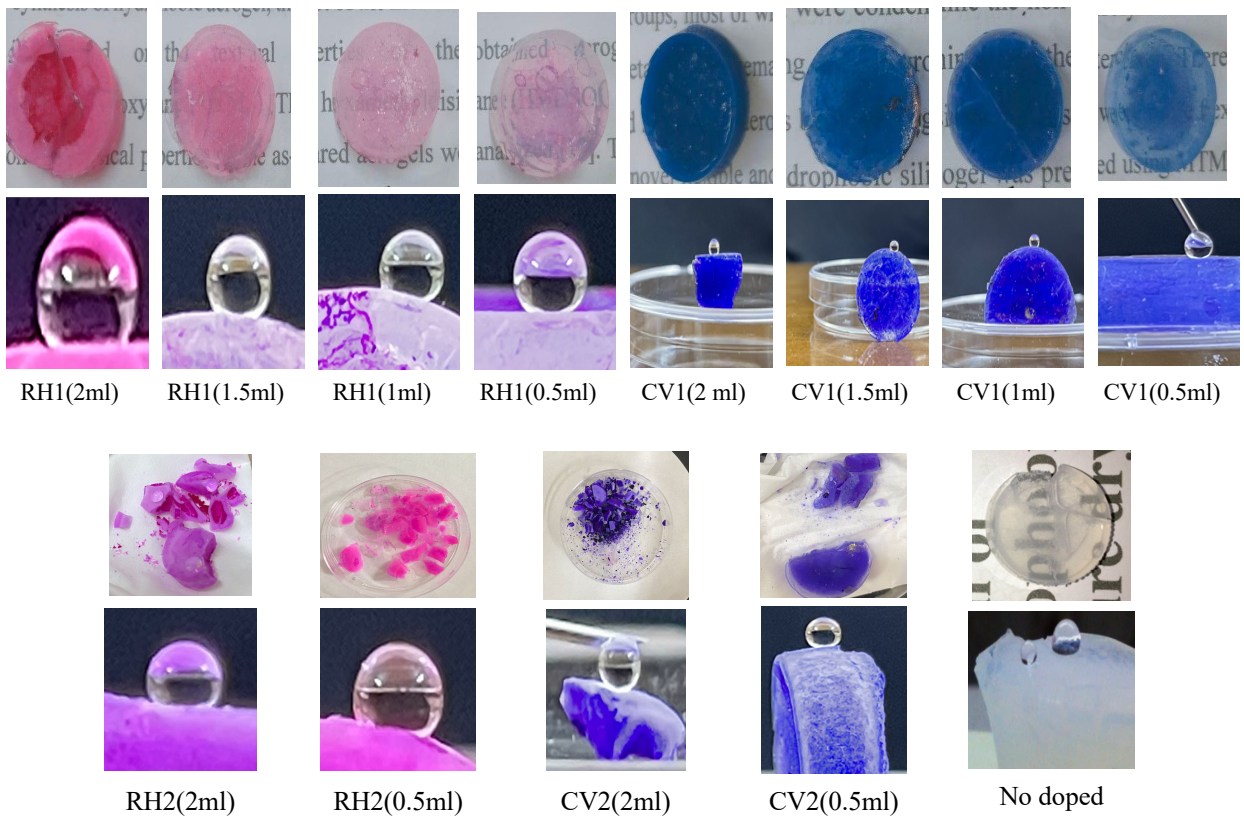

Fig. 6. Photographic images of doped silica aerogel prepared in different ways, RH1and CV1 with (0.5,1, 1.5, 2 ml) and RH2 and CV2 with (0.5 and 2 ml) and no doped

4. Conclusion

Hydrophobic silica aerogel doped with two dye lasers was efficaciously manufactured via ambient pressure drying. It was a two-step procedure using an acid-base catalyst. XRD analysis of the prepared silica aerogel established its amorphous nature; no peaks due to the structural nature of silica (amorphous). After vaccination, it was found that laser dyes did not affect this nature. FT-IR studies confirmed the surface modification of the produced silica aerogel. It also supports the samples' hydrophobic nature (without a peak at 1600 cm^{-1}). This hydrophobic mesoporous silica aerogel has exceptional interesting physical properties, including a low density of 0.081 g/cm^3 and a high surface area of 970 m^2/g. Results indicate that the surface chemical modification on dye-doped aerogel was successful since the dye was used as catalysis for modification by replacing the hydroxide band with an alkyl group. The porous nature of silica gel was verified using FE-SEM imaging. The total pore volume of one of the samples is 42.87 cm^3/g, with a surface area of 970 m^2/g and a mean pore diameter of 13.93 nm, as measured by a BET analyzer. The contact angle measurements confirmed the superior hydrophilic properties of the silica aerogel samples. The obtained contact angle (153°) indicates the silica aerogel's superhydrophobic nature, verifying the required surface modifications. Due to its excellent superhydrophobicity and large specific surface area, the resulting silica aerogel has been used in numerous applications, including catalysis, self-cleaning coating materials, oil spill cleanup methods, and insulating materials. Also, this novel material offers tremendous potential in magneto-optical materials and biomedical applications.

Conflicts of interest

The authors do not have any possible conflicts of importance to declare.

ACKNOWLEDGEMENTS

This study was supported by Mustansiriyah University and Phi center for laboratory tests for help.

References

Agergaard, A. H., Sommerfeldt, A., Pedersen, S. U., Birkedal, H., & Daasbjerg, K. (2021) Dual-Responsive Material Based on Catechol-Modified Self-Immolative Poly (Disulfide) Backbones. *Angewandte Chemie, 133*(39), 21713-21719.

Al-Azmi, A. (2021) Efficient synthesis of Triazolo [4, 5-d] pyrimidine-7-carbonitriles and Imidazole-4, 5-dicarbonitriles using Triethylorthoalkylates and their structural characterisation by Single-crystal x-ray diffraction. *Kuwait Journal of Science, 48*(2).

Al-Mothafer, Z., Abdulmajeed, I., & Al-Sharuee, I. (2021) Effect of oxalic acid as a catalyst and dry control chemical additive (dcca) for hydrophilic aerogel base sodium silicate by ambient pressure drying. *Journal of Ovonic Research Vol, 17*(2), 175-183.

Al-sharuee, I. F. (2019) Thermal Conductivity Performance of Silica Aerogel after Exposition on Different Heating under Ambient Pressure. *Baghdad Science Journal, 16*(3 (Suppl.)), 0770-0770.

AL-Sharuee, I. F. (2021) Specifications study of Hydrophobic Silica Aerogel Doped with Rhodamine 6G Prepared via Sub-Critical Drying Technique. *Iraqi Journal of Science*, 483-489.

Al-sharuee, I. F., & Mohammed, F. H. (2019) *Investigation study the ability of superhydrophobic silica to adsorb the Iraqi crude oil leaked in water.* Paper presented at the IOP Conference Series: Materials Science and Engineering.

Al-Sharueez, I. F., & Twej, W. (2017) Study the Effect of Doping with Chromium Chloride on Silica Aerogel Properties Prepared with Ambient Pressure. *IOSR Journal of Applied Physics, 9*, 28-32.

Anderson, A. M., & Carroll, M. K. (2011) Hydrophobic silica aerogels: review of synthesis, properties and applications. *Aerogels handbook*, 47-77.

Aqeel, T., Greer, H. F., & Bumajdad, A. (2018) Novel synthesis of crystalline mesoporous tin dioxide doped with nanogold. *Kuwait Journal of Science, 45*(2).

Berardi, U., & Zaidi, S. M. (2019) Characterization of commercial aerogel-enhanced blankets obtained with supercritical drying and of a new ambient pressure drying blanket. *Energy Buildings, 198*, 542-552.

Cao, J., Lu, H., Yang, M., Wang, Q., Wei, Z., & Li, J. (2018) Luminescent Rhodamine 6G/silica hybrid nanofibers with potential temperature sensing ability. *Journal of Non-Crystalline Solids, 482*, 40-45.

Chandradass, J., Kang, S., & Bae, D.-s. (2008) Synthesis of silica aerogel blanket by ambient drying method using water glass based precursor and glass wool modified by alumina sol. *Journal of Non-Crystalline Solids, 354*(34), 4115-4119.

De Nicola, F., Castrucci, P., Scarselli, M., Nanni, F., Cacciotti, I., & De Crescenzi, M. (2015) Exploiting the hierarchical morphology of single-walled and multi-walled carbon nanotube films for highly hydrophobic coatings. *Beilstein Journal of Nanotechnology, 6*(1), 353-360.

Guo, Z., Yang, R., Wang, T., An, L., Ren, S., Zhou, C., & Engineering. (2021) Cost-effective additive manufacturing of ambient pressure-dried silica aerogel. *Journal of Manufacturing Science, 143*(1).

Huang, D., Guo, C., Zhang, M., & Shi, L. (2017) Characteristics of nanoporous silica aerogel under high temperature from 950° C to 1200° C. *MaterialsDesign, 129*, 82-90.

Huang, X., Liu, J.-X., Shi, F., Yu, L., & Liu, S.-H. (2016) Ambient pressure drying synthesis of Cs0. 33WO3/SiO2 composite aerogels for efficient removal of Rhodamine B from water. *Materials Design, 110*, 624-632.

Illescas, J. F., & Mosquera, M. J. (2011) Surfactant-synthesized PDMS/silica nanomaterials improve robustness and stain resistance of carbonate stone. *The Journal of Physical Chemistry C, 115*(30), 14624-14634.

Krause, R. G., & Goldring, J. D. (2019) Crystal violet stains proteins in SDS-PAGE gels and zymograms. *Analytical biochemistry, 566*, 107-115.

Li, M., Jiang, H., Xu, D., Hai, O., & Zheng, W. (2016) Low density and hydrophobic silica aerogels dried under ambient pressure using a new co-precursor method. *Journal of Non-Crystalline Solids, 452*, 187-193.

Linhares, T., de Amorim, M. T. P., & Durães, L. (2019) Silica aerogel composites with embedded fibres: a review on their preparation, properties and applications. *Journal of Materials Chemistry A, 7*(40), 22768-22802.

Maleki, H. (2016) Recent advances in aerogels for environmental remediation applications: A review. *Chemical Engineering Journal, 300*, 98-118.

Mosquera, M. J., de los Santos, D. M., & Rivas, T. (2010) Surfactant-synthesized ormosils with application to stone restoration. *Langmuir, 26*(9), 6737-6745.

Pierre, A. C., & Rigacci, A. (2011) SiO 2 aerogels. In *Aerogels handbook* (pp. 21-45): Springer.

Raissi, S., Younes, M., & Ghorbel, A. (2010) Synthesis and characterization of aerogel sulphated zirconia doped with chromium: n-hexane isomerization. *Journal of Porous Materials, 17*(3), 275-281.

Rao, A. V., Nilsen, E., & Einarsrud, M.-A. (2001) Effect of precursors, methylation agents and solvents on the physicochemical properties of silica aerogels prepared by atmospheric pressure drying method. *Journal of Non-Crystalline Solids, 296*(3), 165-171.

Ren, C., Li, J., Chen, X., Hu, Z., & Xue, D. (2007) Preparation and properties of a new multifunctional material composed of superparamagnetic core and rhodamine B doped silica shell. *Nanotechnology, 18*(34), 345604.

Shen, C. A., Bialas, D., Hecht, M., Stepanenko, V., Sugiyasu, K., & Würthner, F. (2021) Polymorphism in Squaraine Dye Aggregates by Self-Assembly Pathway Differentiation: Panchromatic Tubular Dye Nanorods versus J-Aggregate Nanosheets. *Angewandte Chemie, 133*(21), 12056-12065.

Shi, F., Wang, L., & Liu, J. (2006) Synthesis and characterization of silica aerogels by a novel fast ambient pressure drying process. *Materials Letters, 60*(29-30), 3718-3722.

Štengl, V., Bakardjieva, S., Šubrt, J., & Szatmary, L. (2006) Titania aerogel prepared by low temperature supercritical drying. *mesoporous materials, 91*(1-3), 1-6.

Sui, R., Liu, S., Lajoie, G. A., & Charpentier, P. A. (2010) Preparing titania aerogel monolithic chromatography columns using supercritical carbon dioxide. *Journal of separation science, 33*(11), 1604-1609.

Wang, W., Li, Y., Sun, M., Zhou, C., Zhang, Y., Li, Y., & Yang, Q. (2012) Colorimetric and fluorescent nanofibrous film as a chemosensor for Hg 2+ in aqueous solution prepared by electrospinning and host–guest interaction. *Chemical Communications, 48*(48), 6040-6042.

Wiener, M., Reichenauer, G., Braxmeier, S., Hemberger, F., & Ebert, H.-P. (2009) Carbon aerogel-based high-temperature thermal insulation. *International journal of Thermophysics, 30*(4), 1372-1385.

Yun, S., Luo, H., & Gao, Y. (2014) Superhydrophobic silica aerogel microspheres from methyltrimethoxysilane: rapid synthesis via ambient pressure drying and excellent absorption properties. *RSC Advances, 4*(9), 4535-4542.

Submitted: 17-05-2022
Revised: 26-07-2022
Accepted: 14-08-2022
DOI: 10.48129/kjs.20549